PAPER Special Section on Recent Technologies of Microwave and Millimeter-Wave Devices

Proposal of Switching Speed Reduction Method Using Chaotic Spreading Sequence in Direct Optical Switching CDMA Radio-on-Fiber Network and Its Experimental Investigation

Takeshi HIGASHINO[†a)], ***Student Member***, **Katsutoshi TSUKAMOTO**[†], ***Member***, ***and*** **Shozo KOMAKI**[†], ***Fellow***

SUMMARY The direct optical switching CDMA radio-on-fiber network is proposed as multiplexing method for radio base stations in microcell/picocell technologies. In this system, aliasing distortions degrade the received signal quality and decreases the number of connectable radio base stations (RBSs) when the encoding rate becomes lower than the twice of bandwidth of RF signal. This paper proposes the optical switching speed reduction method and clarifies that the chaotic spreading sequences can suppress the aliasing distortion without additional processing at the receiver even if the encoding rate becomes lower than the RF signal bandwidth. The effect in switching speed reduction is theoretically investigated and the effect in aliasing distortions suppression is experimentally investigated by using the proposed method.

key words: *radio on fiber, bandpass sampling, code division multiple access, chaotic spreading sequence, M-sequence*

1. Introduction

Fiber-optic microwave and millimeter-wave RF signal transmission (Radio-on-Fiber) technology has been developed as a strong candidate of broadband wireless access networks and systems [1].

As a multiple access method for radio base stations (RBSs) in microcellular mobile radio fiber-optic transmission system [2], several methods have been studied such as sub-carrier multiple access [3], [4], time division multiple access [5], [6], and the use of distinct wavelength in optical frequency domain (wavelength division multiplexing) [7], [8].

Optical code division multiple access (CDMA) method is another candidate. We have been proposed direct optical switching (DOS)-CDMA radio-on-fiber network [9], [10]. In this system, improved processing gain and maximum connectable RBS can be easily obtained by using broadband optical switching devices for spreading RF signals into optical domain compared with the conventional electrical CDMA system [11]. At the DOS-CDMA transmitter, an optical carrier is intensity modulated according to RF signal amplitude. The obtained optical signal is on-off encoded by the use of photonic switch. An external intensity modulator is used as the photonic switch. A spreading sequence is periodically mapped into an optical on-off intensity pulsed IM (Intensity Modulation) signal. At the optical polarity reversing correlator (OPRC) receiver, two optical switches and a balanced mixing photodetector perform de-spreading. After the de-spreading processing, the original RF signal is regenerated by the use of the bandpass filter (BPF). In order to avoid aliasing distortion, the encoding rate* at the transmitter has to at least be higher than twice of bandwidth of RF signal, which is known well as bandpass sampling theorem [12]–[14]. In case that the encoding rate is equal to the twice of bandwidth of the RF signal, the switching speed becomes much higher than the twice of bandwidth of RF signal. Thus the switching speed reduction technique is the important issue in mitigating the required specifications of optical switching device. When the encoding rate becomes lower than the twice of bandwidth of RF signal, aliasing distortions degrade the received signal quality and decrease the number of connectable RBSs. Reference [15] described about the construction of aliasing canceller filter avoiding the quality deterioration of received signal due to the aliasing which is caused by the expansion of spreading sequence period. The signal reconstruction processing to avoid aliasing, however, is complicated [14]–[16].

For DSSS (Direct Sequence/Spread Spectrum) communication system, chaotic binary sequences have the same properties as well as Gold sequence or Kasami sequence in even- and odd-correlation among spreading sequences [17], [18]. The chaotic spreading sequences [19], [20] potentially have a large number of spreading sequences. This paper proposes the application of chaotic spreading sequences to reduce switching speed and clarifies that the chaotic spreading sequence is effective in aliasing distortion suppression [21] without additional processing at the receiver. This paper theoretically and experimentally investigates the aliasing distortion suppression by using the proposed method.

The rest of this paper is organized as follows. In Sect. 2, we show the principle of interference suppression of DOS-CDMA system. The RF signals which are bandpass sampled by spreading sequence are investigated theoretically. Section 3 shows the chaotic spreading sequence generation method used in this paper and shows the switching speed reduction impact when using proposed chaotic spreading sequences compared to that when using M-sequences in terms

Manuscript received October 30, 2004.
Manuscript revised January 24, 2005.

[†]The authors are with the Department of Communications, Graduate School of Engineering, Osaka University, Suita-shi, 565-0871 Japan.
a) E-mail: higa@roms.comm.eng.osaka-u.ac.jp

DOI: 10.1093/ietele/e88–c.7.1475

*The encoding rate denotes the repetition rate of spreading sequence, and its value is reciprocal of spreading sequence period.

of numerically calculated CDR (carrier-to-distortion power ratio) and SDR (signal-to-distortion power ratio). In Sect. 4, we experimentally investigate CDR and SER (symbol error rate) performances compared to those when using the M-sequence. Section 5 concludes this paper.

2. DOS-CDMA Radio on Fiber Network

2.1 Configuration

Figure 1 shows the configuration of the DOS-CDMA. RF signals, $r(t)$, which are received at RBS intensity modulate the LD (Laser Diode). The obtained IM signal is on-off encoded at the photonic switch (PSW) driven by the spreading sequence, c_i, which is assigned to RBS$_i$. This on-off encoding at the PSW corresponds to the natural bandpass sampling of RF signal. The obtained IM/CDMA signal is multiplexed and transmitted to the control station (CS). Received optical signal is correlated in optical domain by using Optical Polarity-Reversing Correlator (OPRC) [10] receiver. The output of OPRC is obtained by the subtraction of the lower branch's output from upper branch's one electrically. The signal power is reduced by the subtraction for the interference signal only, but the desired signal has no power-reduction because of de-spreading due to the invert sequence at lower branch in the OPRC. Finally, on-off pulsed RF signal is interpolated by the use of BPF in order to obtain the original RF signal.

2.2 Analysis of Bandpass Sampled RF Signal by the Spreading Sequence

An RF signal $r(t)$ with a carrier f_{RF} is written by

$$r(t) = \mathrm{Re}\left\{g(t)e^{j2\pi f_{RF}t}\right\}, \tag{1}$$

where $g(t)$ is the complex baseband signal which has a two-sided bandwidth B_{RF}. The waveform of spreading sequence

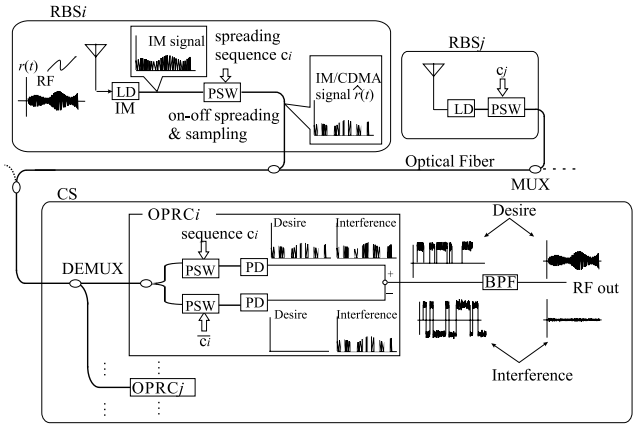

RBS : Radio base station
RF : radio frequency
IM : intensity-modulation
LD : Laser diode
PSW : photonic switch
CS : Control station
MUX : multiplexer
PD : photodetector
OPRC : optical polarity reversing correlator
BPF : Bandpass filter

Fig. 1 Configuration of DOS-CDMA.

which is allocated to RBS$_i$, $s_i(t)$, is represented as

$$s_i(t) = \sum_{m=0}^{L-1} c_i(m) \cdot p_{T_c}(t - mT_c), \tag{2}$$

where $c_i(m) \in \{0, 1\}$ is the m-th chip value. L is spreading sequence length. The sequence length denotes the number of chips in c_i. $p_{T_c}(t)$ is a chip pulse waveform whose height and width are 1 and T_c, respectively. $p_{T_c}(t)$ is represented as follows

$$p_{T_c}(t) = \begin{cases} 1 & |t| \le \frac{T_c}{2} \\ 0 & |t| > \frac{T_c}{2} \end{cases} . \tag{3}$$

The example of spreading sequence waveform is shown in the left side of Fig. 3(a). The spectrum, $P_{T_c}(f)$, of $p_{T_c}(t)$ becomes symmetric about $f = 0$ and the zero points appear at intervals of $1/T_c$. To interpolate an original RF signal from pulsed one at the BPF output without aliasing, the spreading sequence period T_s must be shorter than the required maximal sampling period. This condition is represented as follows [12],

$$T_s = \frac{1}{f_s} \le \frac{1}{2B_{RF}}, \tag{4}$$

where, in this paper, f_s is called as encoding rate.

At the receiver, the signal of subtractor output in front of the BPF, $\hat{r}(t)$, is

$$\hat{r}(t) = r(t) \cdot \sum_{k=-\infty}^{\infty} s_i(t - kT_s) \cdot \left\{s_j(t - kT_s) - \overline{s_j(t - kT_s)}\right\}, \tag{5}$$

where $s_j(t)$ is the j-th receiver's spreading sequence waveform. $\overline{s_j(t)}$ denotes the logical inverted spreading sequence waveform which drives the PSW at lower branch in the OPRC. The $\overline{s_j(t)}$ is represented as

$$\overline{s_j(t)} = \sum_{m=0}^{L-1} \overline{c_j(m)} p_{T_c}(t - mT_c). \tag{6}$$

The $\hat{r}(t)$ is a summation of sampled RF signal by L uniform sampling pulse streams with its period of T_s, and it can be rewritten by

$$\hat{r}(t) = \sum_{m=0}^{L-1} \hat{r}_m(t),$$
$$\hat{r}_m(t) = c_i(m) \cdot \left(c_j(m) - \overline{c_j(m)}\right) \cdot r(t) \cdot \sum_{k=-\infty}^{\infty} \cdot p_{T_c}(t - mT_c - kT_s). \tag{7}$$

Let $G(f)$ denotes the spectrum of $g(t)$. The $\hat{R}(f)$ denotes the spectrum of $\hat{r}(t)$. It is represented as [14], [16]

$$\hat{R}(f) = \frac{1}{2}\hat{G}(f - f_{RF}) + \frac{1}{2}\hat{G}^*(-f - f_{RF}), \tag{8}$$

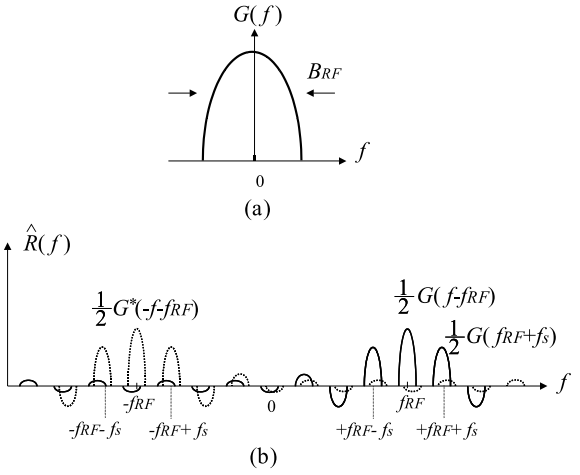

Fig. 2 Schematic diagram of Eqs. (8)–(10). (a) Frequency spectrum of baseband signal $g(t)$. (b) Frequency spectrum of bandpass sampled RF signal $r(t)$ with its bandwidth of B_{RF}. The f_{RF} and f_s are center frequency of $r(t)$ and the encoding rate, respectively.

$$\hat{G}(f) = \sum_{m=0}^{L-1} \hat{G}_m(f), \tag{9}$$

$$\hat{G}_m(f) = c_i(m) \cdot \left\{ c_j(m) - \overline{c_j(m)} \right\} \cdot \frac{T_c}{T_s} \cdot \sum_{k=-\infty}^{\infty} \frac{\sin\left(k\pi \frac{T_c}{T_s}\right)}{k\pi \frac{T_c}{T_s}} \cdot G\left(f - \frac{k}{T_s}\right) e^{-j2\pi k \frac{m}{L}}. \tag{10}$$

Figure 2 shows the schematic diagram of Eqs. (8)–(10).

Figure 2(a) shows the frequency spectrum of baseband signal $g(t)$. Figure 2(b) shows the frequency spectrum of bandpass sampled RF signal $r(t)$ whose bandwidth is B_{RF}. The dashed spectrum is the imaginary spectrum which is generated in the negative frequency domain due to the bandpass sampling. The alias spectrums are located at equally spaced by f_s=1/T_s. The envelope of $\hat{R}(f)$ is weighted by frequency-shifted sinc function. In Eqs. (9) and (10), since $\hat{G}(f)$ is summation of $\hat{G}_m(f)$ for m, the first factor, $c_i(m)\cdot(c_j(m)-\overline{c_j(m)}$, in Eq. (10) becomes correlation value between the c_i and the bipolar version of c_j, and the last term (the term of exponential) in Eq. (10) are composed in complex plane. Thus, the $\hat{G}(f)$ is rewritten by

$$\hat{G}(f) = \theta_{c_i,\chi(c_j)}(\tau) \cdot \frac{T_c}{T_s} \cdot \sum_{k=-\infty}^{\infty} \frac{\sin\left(k\pi \frac{T_c}{T_s}\right)}{k\pi \frac{T_c}{T_s}} \cdot G\left(f - \frac{k}{T_s}\right) \cdot \phi(k), \tag{11}$$

$$\phi(k) = \sum_{\{c_i(m)\cdot c_j(m)=1\}} e^{-j2\pi k \frac{m}{L}} - \sum_{\{c_i(m)\cdot \overline{c_j(m)}=1\}} e^{-j2\pi k \frac{m}{L}}, \tag{12}$$

where $\theta_{c_i,\chi(c_j)}(\tau)$ is the cross-correlation function between {0,+1}-valued sequence, c_i, and {−1, +1}-valued sequence, $\chi(c_j)$, in the DOS-CDMA system [22] where the $\chi(c(m))$=2·$c(m)$ − 1. $\theta_{c_i,\chi(c_j)}(\tau)$ is represented as follows,

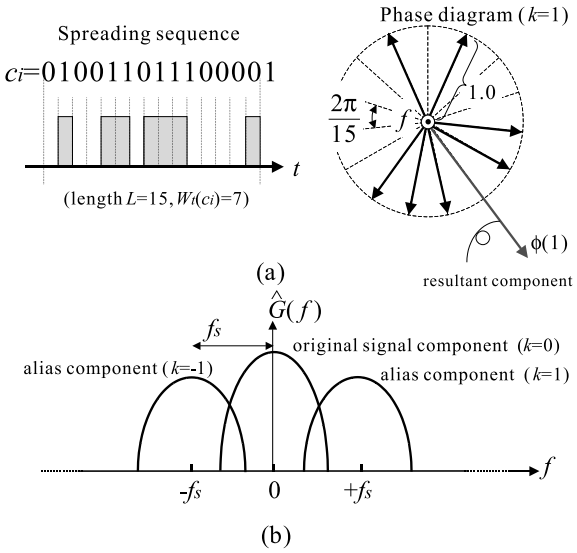

Fig. 3 Schematic diagrams of Eqs. (2), (11) and (15). (a) An example of spreading sequence waveform, s_i and a geometrical representation of phase diagram in Eq. (15). Code sequence, c_i, is 010011011100001. Absolute value and argument of resultant, $\phi(1)$, are 2.0 and 140.8 [deg], respectively. (b) Equivalent lowpass frequency spectrum of bandpass sampled RF signal, $\hat{G}(f)$ ($|k|\leq 1$).

$$\theta_{c_i,\chi(c_j)}(\tau) = \sum_{m=0}^{L-1} c_i(m) \cdot \chi\left(c_j(m+\tau)\right), \quad (0 \leq \tau \leq L-1), \tag{13}$$

where τ is the unit chip delay. In Eq. (11), $\phi(k)$ is the resultant component of exponential term in complex vector format. The first and second terms in Eq. (12) denote the aggregation of phase spectrum which pass through the upper and lower branch at the OPRC, respectively. When the de-spreading sequence $c_j(t)$ is equall to $c_i(t)$ and $\tau = 0$, $c_i(c_i - \overline{c_i}) = c_i$, thus

$$\theta_{c_i,\chi(c_i)}(0) = W_t(c_i), \tag{14}$$

$$\phi(k) = \sum_{\{c_i(m)=1\}} e^{-j2\pi k \frac{m}{L}}, \tag{15}$$

where $W_t(c_i)$ is the Hamming weight of code word, c_i, corresponds the number of '1' in c_i.

Figure 3 shows the schematic diagram of Eqs. (2), (11) and (15). Figure 3(a) shows an example spreading sequence, c_i=010011011100001, and Fig. 3(b) shows the geometrical representation of phase diagram. The sequence length and the Hamming weight are 15 and 7, respectively. In this figure, $\phi(k)$ is the summation of complex unit vectors whose argument depends on the time position of a sampling pulse in the sequence c_i such that $c_i(m) = 1$. The $|\phi(1)|$ of 2.0 and $\angle\phi(1)$ of 140.5 degree are calculated according to Eq. (15). Figure 3(b) shows the equivalent lowpass frequency spectrum of bandpass sampled RF signal, $\hat{G}(f)$ with ($|k| \leq 1$). The spectrum components for $k = 0$ represent the original signal, and for $k \neq 0$ represent the alias spectrums. Alias spectrums are evenly located by f_s in the frequency domain and each amplitude of $\hat{G}(f)$ is weighted by the $|\phi(k)|$ which

is found in Eq. (11). Thus, the alias can be suppressed by using specific spreading sequence with small $|\phi(k)|$. The $|\phi(k)|$ is found the even function for k, such that $|\phi(-k)|=|\phi(k)|$. The $|\phi(k)|$ has a maximum value of $W_t(c_i)$ when k=0, and has positive real numbers less than $W_t(c_i)$ when $k\neq 0$. These values are unique identity for the sampling sequence, c_i, and these values have no change for cyclically chip-shifted version of the same sequence.

2.3 Investigation of Aliasing Distortion

Let r denotes the encoding rate to bandwidth ratio as a switching speed reduction indication,

$$r \triangleq \frac{f_s}{B_{RF}}. \tag{16}$$

Figure 4 shows the dominative distortions depend on the r. In the case of $1 \leq r \leq 2$, the distortion is mainly caused by the imaginary spectrums which are generated from $-f_{RF}$ as shown in Fig. 4(a). In the case of $0 < r < 1$, the spectrums generated from both $-f_{RF}$ and f_{RF} cause aliasing as shown in Fig. 4(b). The received signal quality is deteriorated when the alias spectrums overlap the original signal.

• Case $1 \leq r \leq 2$

The k-th alias spectrums generated from $-f_{RF}$ which overlap the original signal are satisfied as

$$k_{min} \leq k \leq k_{max}, \tag{17}$$

$$k_{min} = \left\lceil \frac{2f_{RF} - B_{RF}}{f_s} \right\rceil, \tag{18}$$

$$k_{max} = \left\lfloor \frac{2f_{RF} + B_{RF}}{f_s} \right\rfloor, \tag{19}$$

and positioned at $-f_{RF} + kf_s$ in frequency domain. These spectrums are the source of distortion. $\lfloor x \rfloor$ represents equal or maximal integer number less than x. $\lceil x \rceil$ represents equal or minimal integer number more than x.

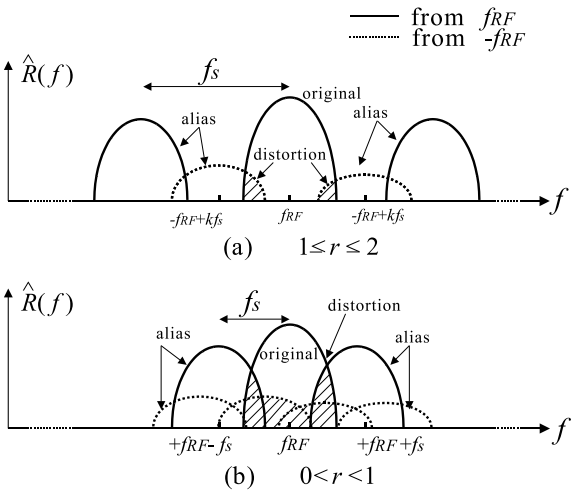

Fig. 4 Frequency spectrum of bandpass sampled RF signal with its encoding rate of f_s and relationship between r and spectrum overlap. (a) In case of $1 \leq r \leq 2$. (b) In case of $0 < r < 1$.

Figure 5 shows some conditions for signal-to-distortion power ratio (SDR) calculation. In order to estimate the maximum degradation of SDR due to the aliasing, it is assumed that the shape of spectrum is rectangular and $|\phi(k)| = W_t(c_i)$ on every k. The extremum points of envelope function are used in order to estimate the lower bound of SDR as shown in Fig. 5(b).

SDR is written by

$$SDR = \frac{B_{RF}}{\sum_{k=k_{min}}^{k_{max}} l_{overlap} \cdot \left(\frac{\sin\left(k\pi \frac{T_c}{T_s}\right)}{k\pi \frac{T_c}{T_s}} \right)^2}, \tag{20}$$

where $l_{overlap}$ denotes the bandwidth of overlap region between the original signal and alias spectrum as shown in Fig. 5. The $l_{overlap}$ is written by

$$l_{overlap} = \begin{cases} f'_u - f_l & \left(f_{RF} \geq -2f_{RF} + \frac{k}{T_s}\right) \\ f_u - f'_l & \left(f_{RF} < -2f_{RF} + \frac{k}{T_s}\right). \end{cases} \tag{21}$$

Let f_c=$1/T_c$ is the chip rate with its pulse width of T_c, and p denotes the ratio of f_c to f_{RF},

$$p \triangleq \frac{f_c}{f_{RF}}. \tag{22}$$

Figure 6 shows the relationship between p and lower bound SDR in the case of f_{RF}=1.9 GHz and B_{RF}=300 kHz. Lower bound is estimated by using extremal values of $\sin(\pi f T_c)/(\pi f T_c)$ where $f = (2n+1)/2T_c$ for $n = \pm 1, \pm 2, \ldots$ [12]. It is found that the SDR degrades seriously due to aliasing when $p \to 1$. In the Fig. 6, each SDR has -20 dB deterioration per decade of increase in p because the square value of $(\sin x)/x$ at these extremal values are approximated to $1/x^2$. In case of r= 1, SDR has lowest performance because alias spectrums are closely spaced in frequency domain. The SDR has more than 70 dB in the case of $p \leq 10^{-3}$.

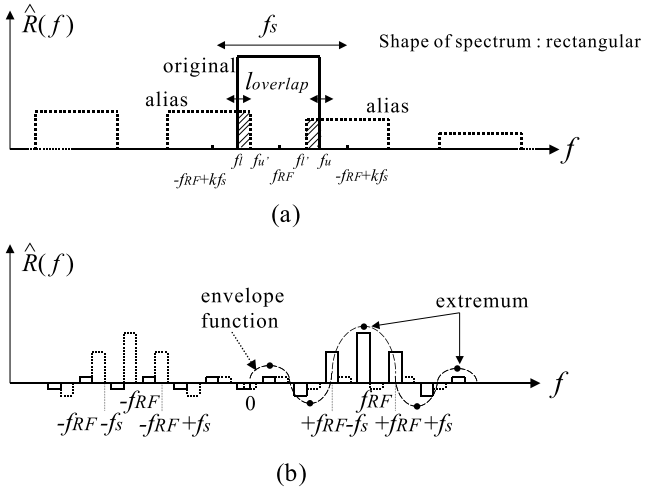

Fig. 5 Frequency spectrum of bandpass sampled RF signal of $r(t)$ and some conditions for SDR calculation in case of $1 \leq r \leq 2$. (a) The spectrum shape is rectangular. (b) Extremum points of envelope function are used for the SDR calculation.

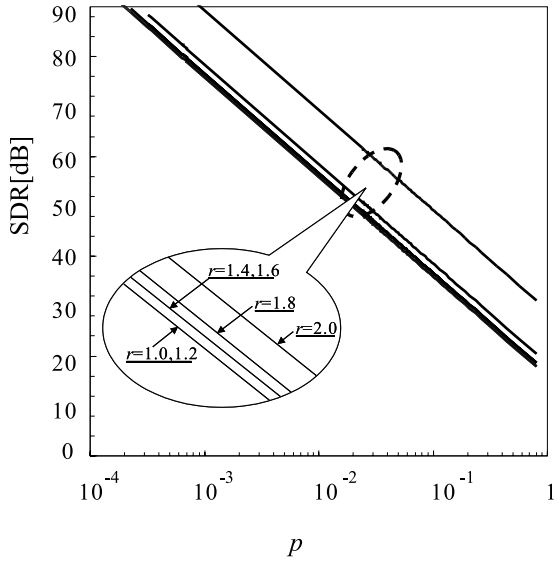

Fig. 6 Relationship p versus SDR (f_{RF}=1.9 GHz, B_{RF}=300 kHz).

It is found that the distortion is almost negligible small when $p \leq 10^{-3}$.

• Case $0 < r < 1$

Figure 4(b) shows spectral position in case of $0<r<1$. It is assumed that the SDR degradation by aliasing distortion generated from $-f_{RF}$ is negligible small when $p \leq 10^{-3}$. Thus, in this case, the power of distortion should be estimated considering the alias generated from f_{RF} only.

The k-th alias spectrums generated within signal bandwidth are satisfied as

$$k = \pm 1, \ldots, \pm (\lceil B_{RF}/f_s \rceil - 1). \tag{23}$$

In the range of k which satisfied as

$$\left(\frac{\sin k\pi \frac{T_c}{T_s}}{k\pi \frac{T_c}{T_s}} \right)^2 \simeq 1, \tag{24}$$

the contrast of absolute value of $\phi(0)$ and the other $\phi(k)$ are approximated to CDR on every k and it is written by

$$CDR(k) = 20 \log \frac{|\phi(0)|}{|\phi(k)|} \quad [\text{dB}]. \tag{25}$$

In Fig. 3, the $CDR(1)$ is calculated as 7.0/2.0=3.5 ($\simeq$ 10.9 dB).

3. Chaotic Spreading Sequence Generation

It is seen from Eq. (11) that alias power at $f=f_{RF}+k/T_s$ strongly depends on $|\phi(k)|$ except the spectrum at center frequency of $f_{RF}(k=0)$. The value of $|\phi(k)|$ is determined by time position of sampling pulse where a chip value of $c_i(m)$=1. As a simple example, it is known that, from Eq. (15), the value of $|\phi(k)|$ is able to be zero when the sampling pulses are positioned as aliasing amplitude spectrums are balanced out. However, these spectrums can not be existed. This is because a local periodicity within the spreading sequence period dominates the characteristics of $\phi(k)$.

Table 1 Relationship between k and $|\phi(k)|$ for desired signal used in the experiment of Fig. 9. CDR(k) is calculated by Eq. (25).

	k	0	1	2	3	4
M-seq. (127)	$\|\phi(k)\|$	64.0	5.66	5.66	5.66	5.66
	CDR(k) [dB]		21.07	21.07	21.07	21.07
Chaos-seq. (127)	$\|\phi(k)\|$	61.0	0.874	0.220	1.887	5.352
	CDR(k) [dB]		36.87	48.86	30.19	21.14

Table 2 Relationship between k and $|\phi(k)|$ used in the experiment of Fig. 10. CDR(k) is calculated by Eq. (25).

	k	0	1	2	3	4
M-seq. (63)	$\|\phi(k)\|$	32.0	4.00	4.00	4.00	4.00
	CDR(k) [dB]		18.1	18.1	18.1	18.1
Chaos-seq. (63)	$\|\phi(k)\|$	36.0	0.077	0.295	0.331	3.60
	CDR(k) [dB]		53.4	41.7	40.7	20.0

Therefore, in order to exclude that the local periodicity is generated within the spreading sequence period, the chaotic binary sequences are used as a spreading sequence to multiplexing [19] and to suppress aliasing distortion.

The $|\phi(k)|$ is a unique value of a spreading sequence, and it is constant even if the spreading sequence is shifted by any chip cyclically. From the viewpoints of multiplexing and aliasing distortion suppression, following two characteristics are desired for the spreading sequence when the encoding rate becomes lower than the signal bandwidth; (1) The $|\phi(k)|$ ($k \neq 0$, $k \leq \lceil B_{RF}/f_s \rceil - 1$) of desired spreading sequence is relative small thus not to degrade the signal quality. (2) Since the electrical waveform before the integrator at the receiver is multiplication format between $r(t)$ and $c_i(c_j - \overline{c_j})$, the $\phi(k)$ of $c_i(c_j - \overline{c_j})$ are also relative small enough thus not to degrade the number of multiplexing. The chaotic binary spreading sequences which satisfy above characteristics to be possible, are selected from infinite spreading sequences generated from chaotic map as follows; A m-th chip value of sequence, $c_i(m)$, ($0 \leq m \leq L-1$), is generated from time series x_m in the real-number domain X which is settled $X = [0, 1]$. We take a logistic map, $x_{m+1}=4x_m(x_m - 1)$, ($0 \leq m \leq L-1$), [20] where L is arbitrary sequence length. The m-th chip value of $c_i(m)$, ($0 \leq m \leq L-1$), are '1' or '0' when $x_m > 0.5$ or $x_m \leq 0.5$, respectively. The different initial values (x_0) generates different sequence.

First, a spreading sequence generation on the basis of aliasing distortion suppression for a desired RF signal is performed, and the another spreading sequence generation is performed considering both interference suppression and aliasing distortion suppression for interference RF signal.

• Alias suppression for a desired RF signal

Table 1 shows the relationship between k and CDR(k) of M-sequence (M-seq.) and chaotic spreading sequence (Chaos-seq.) with their sequence length are 127 used in the alias suppression experiment. The CDR(k) shown in Table 1 is calculated by Eq. (25). Table 2 shows the relationship between k and $|\phi(k)|$ in cases of M-seq. and Chaos-seq. with their sequence length are 63. The Chaos-seq. is generated in consideration of alias suppression for the alias components of $|k| \leq 3$.

Table 3 Relationship between k and $|\phi(k)|$ for interference signal used in the experiment of Fig. 11. CDR(k) is calculated by Eq. (25).

	k	1	2	3	4
M-seq. (127)	$\|\phi(k)\|$	7.225	11.12	9.89	4.10
	CDR(k) [dB]	18.95	15.20	16.22	23.87
Chaos-seq. (127)	$\|\phi(k)\|$	2.31	1.24	2.60	6.87
	CDR(k) [dB]	28.41	33.86	27.40	19.09

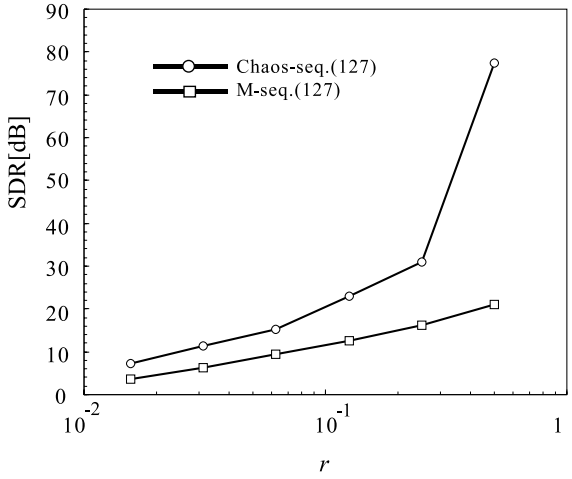

Fig. 7 Relationship between r versus SDR (f_{RF} = 1.9 GHz, B_{RF} = 300 kHz). Chaos-seq. and M-seq. whose CDR properties are shown in Table 1 are used for SDR calculation.

• Alias suppression for interference RF signal

Table 3 shows the relationship between k and $|\phi(k)|$ of multiplied spreading sequence at the OPRC with their sequence length of 127. Figure 7 shows the numerical analysis of relationship between r and SDR which are calculated by using spreading sequences shown in Table 1 in case of $0 < r < 1$. The length of both spreading sequences are 127, respectively. The conditions shown in Fig. 6 are used in SDR calculation. When the required SDR is 20 dB, the encoding rate can be reduce to 2^{-1} and 10^{-1} of the signal bandwidth, B_{RF}, in cases of using M-seq. and Chaos-seq. respectively. It is found that Chaos-seq. can more avoid the deterioration due to the aliasing compared to using the M-seq. even if the encoding rate becomes lower than the RF signal bandwidth.

4. Experiments of Aliasing Distortion Suppression

4.1 Experimental Setup

Figure 8 and Table 4 show the experimental setup and a summary of the specification of devices, respectively. The transmitter consists of Laser Diode (LD) and a $LiNbO_3$ intensity modulator (LN-MOD). The RF signal, generated from the standard signal generator, intensity modulates the LD with its wavelength of 1.3 μm. The IM signal is on-off sampled by the use of LN modulator driven by the rectangular pulse spreading sequences generated from arbitrary waveform code generator1 or 2. The receiver consists of an optical 3 dB coupler, two LN modulators (LN-MOD), an optical delay line (ODL), two optical attenuators (ATT), a balanced mixing PD (BMPD), a bandpass filter (BPF), and an RF amplifier. At the receiver, the received optical signal is divided into two branches by using the 3 dB coupler. The divided optical signals are de-spread by each LN-MOD. The lower side LN-MOD is driven with an inversed spreading sequence. At the BMPD, the de-spread optical signals are photo-detected and electrically subtracted. Then, the desired RF signal is regenerated from the pulsed RF signal and the interference signal is suppressed by the interpolation at the BPF. In this experiment, we use an optical delay line in order to balance the light path length of both branches in OPRC. We also use an optical attenuator in order to balance the optical power of both branches in OPRC.

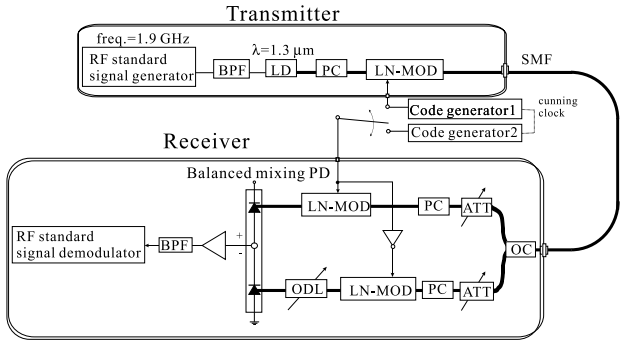

LD : Laser diode
BPF : Bandpass filter
LN-MOD:LN intensity modulater (Photonic SW)
SMF : single mode fiber
OC : 3dB optical coupler
ATT : optical attenuator
ODL : optical delay line
PC: polarization controller

Fig. 8 Experimental setup.

Table 4 Specification of devices used in experiment.

RF standard signal generator	HP ESG-D4000A PHS (RCR STD-28)
RF modulation	$\pi/4$ shift DQPSK
RF carrier frequency	1.9 GHz
output RF power	10 dBm
bandwidth of RF signal	300 kHz
LD module (ORTEL 3541C)	DFB Laser wavelength λ: 1.3 μm output power: 3.4 dBm RIN: −149 dB/Hz mod. gain γ: 0.103 W/A
LN intensity modulator (transmitter) (RAMAR corp.)	insertion loss: 6.1 dB extinction ratio: 35.7 dB V_π: 6.0 Vpp
LN intensity modulator (receiver) (SumitomoTMZ1.3-2.5)	insertion loss 6.0 dB(upp.), 4.4 dB(low.) extinction ratio 33.2 dB(upp.), 32.0 dB(low.) V_π: 1.0 Vpp(upp.), 1.0 Vpp(low.)
PD(NEC NDL5481P1)	responsivity:0.91 A/W
BPF(receiver)	2nd-order butterworth filter center:1.9 GHz, bandwidth:70 MHz
RF standard signal demodulator	HP 70910A (RF part) HP 89410A (baseband part)

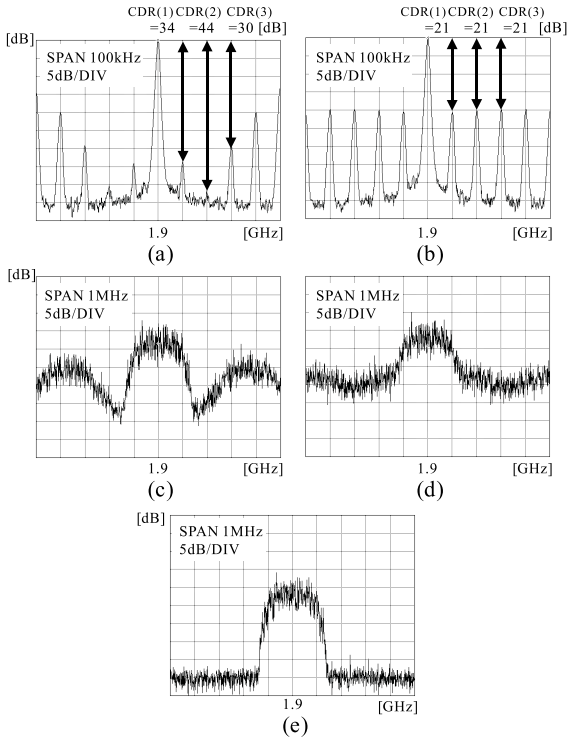

Fig. 9 Observed spectrums of desired signal (L=127, r=1/4). (a) Received CW in case of using Chaos-seq. (b) Received CW in case of using M-seq. (c) Received modulated RF signal in case of using Chaos-seq. (d) Received modulated RF signal in case of using M-seq. (e) Original RF signal.

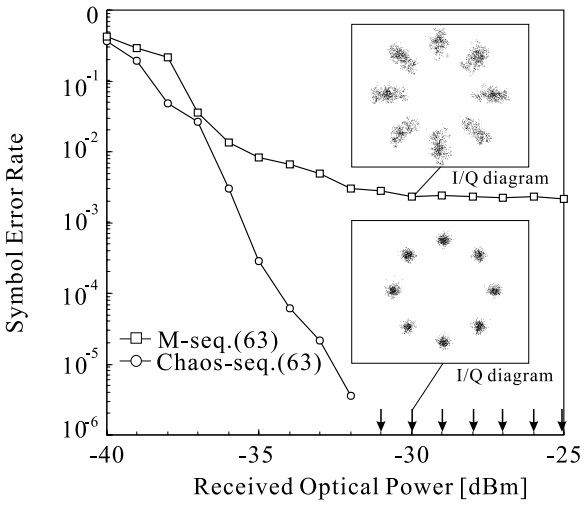

Fig. 10 Symbol error rate versus received optical power (L=63, r=1/4).

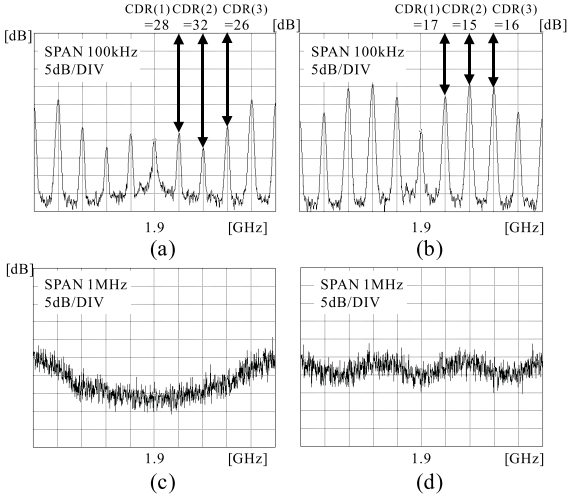

Fig. 11 Observed spectrums of interference signal (L=127, r=1/4). (a) Received CW in case of using Chaos-seq. (b) Received CW in case of using M-seq. (c) Received modulated RF signal in case of using Chaos-seq. (d) Received modulated RF signal in case of using M-seq.

4.2 Results

4.2.1 Aliasing Distortion Sppression for Desired Signal

Figure 9 shows observed spectrums of desired signal in cases of the continuous wave(CW) and modulated RF signal. Obtained CDR(k) ($|k| \leq 4$) in Figs. 9(a) and (b) are close to the calculated ones which were numerically analyzed as shown in Table 1. Figure 9(e) shows the original RF signal. Alias components are adequately suppressed, and original signal spectrum is clearly observed compared to using M-seq. as shown in Figs. 9(c) and (d).

Figure 10 shows the received optical power versus SER (symbol error rate) for desired RF signal. Total number of received symbol is about one million. In cases of f_s=75 kHz (r=1/4) and L=63, alias spectrum corresponding to $1 \leq |k| \leq 3$ are generated within signal bandwidth of 300 kHz. As opposed to the performance limitation due to the distortion was observed in case of using M-seq., stably received I/Q diagrams and improved SER performance of less than 10^{-6} are observed in case of using Chaos-seq.

4.2.2 Aliasing Distortion Suppression for Interference Signal

Figure 11 shows observed spectrums of interference signal in cases of the continuous wave (CW) and modulated RF signal. Obtained CDR(k) ($1 \leq |k| \leq 4$) in Figs. 11(a) and (b) are close to the calculated ones which were numerically analyzed as shown in Table 3. Alias components for interference signal are adequately suppressed compared to using M-seq. as shown in Figs. 11(c) and (d). The validity of numerical analysis in Sects. 2.2 and 2.3 are confirmed by experimental measurements in Sects. 4.2.1 and 4.2.2.

5. Conclusion

This paper has proposed the switching speed reduction method using chaotic spreading sequence to suppress aliasing distortion without additional processing in the receiver even if the encoding rate becomes lower than the RF signal bandwidth in the DOS-CDMA radio on fiber network. Theoretical analysis showed that aliasing distortion is negligi-

ble small in case that $p<10^{-3}$ and $1\leq r\leq 2$. Switching speed reduction effect was also numerically analyzed in cases of using Chaos-seq. and M-seq. as shown in Fig. 7. It is found that the switching speed can be reduce to 10^{-1} for the signal bandwidth by using Chaos-seq. Alias suppression effect is experimentally confirmed by using Chaos-seq. and symbol error rate improvement effect is also confirmed compared to using M-seq. as shown in Fig. 10.

References

[1] S. Komaki, K. Tsukamoto, S. Hara, and N. Morinaga, "Proposal of fiber and radio extension link for future personal communications," Microw. Opt. Technol. Lett., vol.6, no.1, pp.55–60, Jan. 1993.
[2] J. Namiki, M. Shibutani, W. Domon, T. Kanai, and K. Emura, "Optical feeder basic system for microcellular mobile radio," IEICE Trans. Commun., vol.E76-B, no.9, pp.1069–1077, Sept. 1993.
[3] W.I. Way, "Subcarrier multiplexed lightwave system design considerations for subscriber loop applications," J. Lightwave Technol., vol.7, no.11, pp.1806–1818, Nov. 1989.
[4] H. Ogawa, "Microwave and millimeter-wave fiber optic technologies for subcarrier transmission systems," IEICE Trans. Commun., vol.E76-B, no.9, pp.1078–1090, Sept. 1993.
[5] Y. Shoji, K. Tsukamoto, and S. Komaki, "Proposal of radio highway networks using asynchronous time division multiple access," IEICE Trans. Commun., vol.E79-B, no.3, pp.308–315, March 1996.
[6] H. Harada, S. Kajiya, K. Tsukamoto, S. Komaki, and N. Morinaga, "TDM intercell connection fiber-optic bus link for personal radio communication system," IEICE Trans. Commun., vol.E78-B, no.9, pp.1287–1294, Sept. 1995.
[7] C. Lim, A. Nirmalathas, D. Novak, and R. Waterhouse, "Capacity analysis and the merging of a WDM ring fiber-radio backbone incorporating wavelength interleaving with a sectorized antenna interface," IEICE Trans. Electron., vol.E86-C, no.7, pp.1184–1190, July 2003.
[8] T. Kuri and K.I. Kitayama, "Novel channel-selection scheme of dense wavelength division multiplexed millimeter-wave-band radio-on-fiber signals with optical heterodyne detection," IEICE Trans. Electron., vol.E86-C, no.7, pp.1146–1152, July 2003.
[9] S. Park, K. Tsukamoto, and S. Komaki, "Polarity-reversing type photonic receiving scheme for optical CDMA signal in radio highway," IEICE Trans. Electron., vol.E81-C, no.3, pp.462–467, March 1998.
[10] S. Park, K. Tsukamoto, and S. Komaki, "Proposal of direct switching CDMA for cable-to-the-air system and its performance analysis," IEICE Trans. Commun., vol.E81-B, no.6, pp.1188–1196, June 1998.
[11] S. Kajiya, K. Tsukamoto, and S. Komaki, "Proposal of fiber-optic radio highway networks using CDMA method," IEICE Trans. Electron., vol.E79-C, no.1, pp.111–117, Jan. 1996.
[12] H. Taub and D.L. Schilling, Principles of Communication Systems, McGraw Hill International Editions, Electrical and Electronic Engineering Series, 1986.
[13] R.G. Vaughan, N.L. Scott, and D.R. White, "The theory of bandpass sampling," IEEE Trans. Signal Process., vol.39, no.9, pp.1973–1984, Sept. 1991.
[14] A. Kohlenberg, "Exact interpolation of band-limited functions," J. Appl. Phys., vol.24, no.12, pp.1432–1436, Dec. 1993.
[15] K. Kumamoto, K. Tsukamoto, and S. Komaki, "Proposal of higher-order spread spectrum direct optical switching CDMA system," IEICE Trans. Commun., vol.E83-B, no.8, pp.1753–1765, Aug. 2000.
[16] A.J. Coulson, "A generalization of nonuniform bandpass sampling," IEEE Trans. Signal Process., vol.43, no.3, pp.694–704, March 1995.
[17] S. Aoki, K. Yamada, Y. Nose, I. Sasaki, and K. Aoki, "A study on the applicability of chaotic quantized sequences with synchronized bits for SS code," IEICE Technical Report, DSP98-64, SST98-22, CS98-60, July 1998.
[18] T. Kohda and A. Tsuneda "Pseudonoise sequences by chaotic nonlinear maps and their correlation properties," IEICE Trans. Commun., vol.E76-B, no.8, pp.855–862, Aug. 1993.
[19] G. Mazzini, G. Setti, and R. Rovatti, "Chaotic complex spreading sequences for asynchronous DS-CDMA—Part I: System modeling and results," IEEE Trans. Circuits Syst. I, vol.44, no.10, pp.937–947, Oct. 1997.
[20] G.H. Bateni and C.D. McGillem, "A chaotic direct-sequence spread-spectrum communication system," IEEE Trans. Commun., vol.42, no.2/3/4, pp.1524–1527, Feb. 1994.
[21] T. Higashino, K. Tsukamoto, and S. Komaki, "A new spreading code generation method for DOS CDMA RoF system and its experimental investigation," Proc. International Topical Meeting on Microwave Photonics 2003, pp.291–294, Sept. 2003.
[22] T. Higashino, K. Tsukamoto, and S. Komaki, "An experimental investigation of interference suppression in direct optical switching CDM radio-on-fiber system," IEICE Trans. Electron., vol.E86-C, no.7, pp.1159–1166, July 2003.

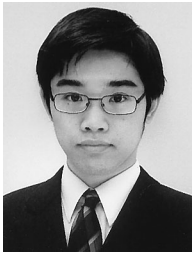

Takeshi Higashino was born in Osaka, Japan in November 11, 1978. He received the B.E. and M.E. degrees in Communications Engineering from Osaka University, Osaka, Japan, in 2001 and 2002 respectively. He is currently pursuing the Ph.D. degree at Osaka University. He is engaging in the research on radio and optical communication systems.

Katsutoshi Tsukamoto was born in Shiga, Japan in October 7, 1959. He received the B.E., M.E. and Ph.D. degrees in Communications Engineering from Osaka University, in 1982, 1984 and 1995 respectively. He is currently an Associate Professor in the Department of Communications Engineering at Osaka University, engaging in the research on radio and optical communication systems. He is a member of IEEE and ITE. He was awarded the Paper Award of IEICE, Japan in 1996.

Shozo Komaki was born in Osaka, Japan, in 1947. He received B.E., M.E. and Ph.D. degrees in Electrical Communication Engineering from Osaka University, in 1970, 1972 and 1983 respectively. In 1972, he joined the NTT Radio Communication Labs., where he was engaged in repeater development for a 20-GHz digital radio system, 16-QAM and 256-QAM systems. From 1990, he moved to Osaka University, Faculty of Engineering, and engaging in the research on radio and optical communication systems. He is currently a Professor of Osaka University. Dr. Komaki is a senior member of IEEE, and a member of the Institute of Television Engineers of Japan (ITE). He was awarded the Paper Award and the Achievement Award of IEICE, Japan in 1977 and 1994 respectively.